# The Ground- and Excited-State ($^1$n$\pi$* and $^1\pi\pi$*) Carboxylic Acid-Catalyzed Proton (Hydrogen Atom)-Transfer Energy Surfaces in 3-Formyl-7-azaindole

**Fa-Tsai Hung***

*The National Hu-Wei Institute of Technology, Yunlin, Taiwan ROC*

**Wei-Ping Hu* and Pi-Tai Chou*,†**

*Department of Chemistry, The National Chung-Cheng University, Chia Yi, Taiwan ROC*

*Received: July 11, 2001; In Final Form: September 11, 2001*

Theoretical approaches on the ground- and excited-state proton (or hydrogen atom) transfer in the 3-formyl-7-azaindole (3FAI)/formic acid dual hydrogen-bonded complex were performed. In the ground state, the analysis of the transition-state geometry led us to conclude a concerted, asynchronous proton-transfer pattern that correlates with the hydrogen-bonding strength. The lowest singlet excited state in the 3FAI/formic acid complex was calculated to be in an n$\pi$* configuration. On the basis of frontier molecular orbital analyses, the n → $\pi$* transition was concluded to originate from the carbonyl lone-pair electrons of the formyl substitute. A highly endergonic proton-transfer reaction barrier of ∼16.7 kcal/mol was calculated in the $^1$n$\pi$* state at the CIS/6-31G(d′,p′) level of theory. The second excited singlet state possesses a $\pi\pi$* configuration in which the excited-state double proton transfer (ESDPT) takes place with a negligible energy barrier. The results provide a theoretical rationalization of the competitive internal conversion/ESDPT mechanism previously proposed for the 3FAI hydrogen-bonded complexes (*J. Phys. Chem. A* **2000**, *104*, 8863).

## 1. Introduction

At the molecular level, the dual hydrogen-bonding dimer of 7-azaindole (7AI) has long been recognized as a simplified model for the hydrogen-bonding base pair of DNA.[1−3] Upon a singlet $\pi \rightarrow \pi^*$ excitation, the 7AI dimer demonstrated the first documented example of the biprotonic transfer reaction, resulting in a large Stokes-shifted tautomer emission (e.g., $\lambda_{max} \approx 480$ nm in cyclohexane).[1] Such an excited-state double proton-transfer (ESDPT) process provides one possible molecular-based interpretation for the mutation due to a "misprint" induced by the proton-transfer tautomerism during replication.[3−5] This in combination with its fundamental importance has led to much research focusing on the dynamics of double proton transfer in the 7AI dimer.[6−27] Conversely, via the formation of 7AI(host)/guest hydrogen-bonded complexes, the spectroscopy and dynamics of 7AI-incorporating guest molecules have also received considerable attention.[28−36] Studies on 7AI complexed using guest molecules such as carboxylic acids, lactams, and amides have revealed prominent ESDPT properties in which the reaction pattern has been classified into two categories on the basis of its chemical aspects.[31c,33b−d] For the catalytic type of reaction (see Figure 1) in which the guest molecule (e.g., acetic acid) remains unchanged during ESDPT, both steady-state and dynamical approaches predicted an ultrafast proton-transfer rate,[33b−d] although experiments on ultrafast dynamics, to our knowledge, have not yet been performed to resolve this issue. In alcohol and water, the dynamics of ESDPT in 7AI and its biorelated analogue 7-azatryptophan have been successfully applied to probe solvation and/or protein dynamics.[28−32,33a,e]

Alternatively, the chemical modification of 7AI to study the substituent effect on ESDPT is also of interest. We have recently reported on spectroscopic and dynamical studies of 3-formyl-7-azaindole (3FAI, see Figure 1).[37] In contrast to the high fluorescence yield in the 7AI monomeric form ($\Phi_f \approx 0.22$ in cyclohexane[31b]), the lack of normal emissions in both the 3FAI monomer and its associated hydrogen-bonded complexes led us to propose that the lowest excited singlet state is in an n$\pi$* configuration. The rate of $S_2(\pi\pi^*) \rightarrow S_1(n\pi^*)$ internal conversion was deduced to be $\sim 4.4 \times 10^{12}$ s$^{-1}$ in cyclohexane.[37] It was further proposed that the proton-transfer reaction in the $S_1$-(n$\pi$*) state is either thermodynamically prohibited or dynamically too slow to compete with other non-proton-transfer deactivation processes. In contrast, the second excited singlet

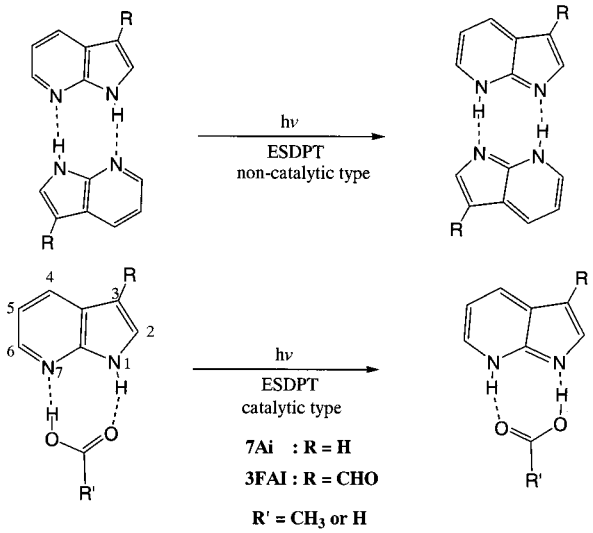


**Figure 1.** The carboxylic acid-catalyzed ESDPT reaction in 7AI and/or 3FAI. Note that experimentally acetic acid was used as the guest molecule,[37] while for simplicity formic acid was applied in this study.

† Current Address: Department of Chemistry, The National Taiwan University, Taipei, Taiwan, ROC.

10.1021/jp012663o CCC: $20.00 
Published on Web 10/19/2001

state possesses a $\pi\pi^*$ configuration in which a fast rate of ESDPT takes place. Accordingly, the dynamics of $S_2(\pi\pi^*) \rightarrow S_1(n\pi^*)$ internal conversion can serve as an internal clock to examine the mechanism of guest-molecule-assisted ESDPT in the $S_2(\pi\pi^*)$ state. For 3FAI in bulk alcohols, the rate of solvent diffusive redistribution (e.g., approximately a few hundred per picosecond in linear-carbon-chain monoalcohols at room temperature[31,32b]) to form a "correct" precursor for ESDPT was concluded to be much slower than the rate of $S_2(\pi\pi^*) \rightarrow S_1(n\pi^*)$ internal conversion. In contrast, for the 3FAI dimer or 3FAI/acetic acid complex possessing intact dual hydrogen bonds, the intrinsic ESDPT rate is fast and thus competes with the $S_2(\pi\pi^*) \rightarrow S_1(n\pi^*)$ internal conversion rate. Accordingly, a prominent proton-transfer tautomer emission band has been resolved in both the 3FAI dimer and the 3FAI/acetic acid complex.[37] Further approaches based on the steady-state quantum yield measurements estimated the rate of ESDPT to be 343 and 187 $fs^{-1}$, respectively, for the 3FAI dimer and 3FAI/acetic acid complex in cyclohexane (298 K). Because the interpretation of the observed ESDPT dynamics in 3FAI relies mainly on the interplay between the $^1\pi\pi^*$ and $^1n\pi^*$ states, further studies regarding the relative energy levels as well as their corresponding proton-transfer potential energy surface (PES) are important. Herein, we report detailed ab initio approaches to the ground- and excited-state formic acid-catalyzed proton (or hydrogen atom) transfer in 3FAI. Our goal is to examine the molecular structures and energy levels of the ground and low-lying singlet excited states in the 3FAI/formic acid complex, particularly their associated potential energy surface (PES) upon executing the proton-transfer reaction. Consequently, a fair comparison can be made between experimental and theoretical approaches.

## 2. Experimental Section

Because only few additional experimental data need to be appended to correlate with the theoretical approach, one can refer to the methodology for steady-state and time-resolved measurements in our preceding report.[37] Details of the pump/probe transient absorption as well as the two-step laser-induced fluorescence technique were elaborated in our previous report.[17] Furthermore, the theoretical approaches using the HF/6-31G(d,p) method to calculate the formation thermodynamics of 3FAI/acetic acid complexes in the ground state were elaborated in our previous report.[37] To avoid complexity and redundancy, our calculation is based on a preexisting 3FAI/formic acid dual hydrogen-bonded complex in which the structures, energetics, and PES upon proceeding with the proton-transfer reaction in both the ground and excited states are involved. The geometry optimization for the ground- and excited-state ($^1n\pi^*$ and $^1\pi\pi^*$) stationary points was performed via either Hartree−Fock (HF)[38,39] or CI singles (CIS)[39b,40] methods incorporating 3-21G(d,p), 6-31G(d′), and 6-31G(d′,p′) atomic basis sets.[41,42] The ground-state stationary points were also optimized using the B3LYP[43,44] hybrid density functional (DFT) method with the 6-31G(d′,p′) basis set. All stationary points were verified by performing vibrational analyses. Vertical excitation energies were calculated using both the CIS and time-dependent (TD)[45] B3LYP methods with 6-31G(d′) or 6-31G(d′,p′) basis sets.

The following sections are organized according to a sequence of steps in which we first performed a detailed examination for the molecular structures and energy levels of the ground and low-lying singlet excited states in the 3FAI/formic acid complex. A fair comparison was then made between the 3FAI/formic acid and 7AI/formic acid complexes. Subsequently, the associated PES during the proton-transfer reaction was calculated. The results in combination with additional experimental data rationalized the previously proposed mechanism in which the lowest-lying $S_{n\pi^*}$ state plays a key role for the observed proton-transfer dynamics in 3FAI hydrogen-bonded complexes.

## 3. Results and Discussion

**3.1. Choice of the 3FAI/Formic Acid System.** The 3FAI/formic acid dual hydrogen-bonded complex offers several preferences over the 3FAI dimer or other corresponding hydrogen-bonded complexes when used as a model for the theoretical approach. First, a large association constant ($K_a$) of $2 \times 10^5$ $M^{-1}$ upon forming the 3FAI/acetic acid complex was reported in cyclohexane.[37] It is reasonable to assume a similar $K_a$ value so that the 3FAI/formic acid dual hydrogen-bonded complex should exist prevalently in gas as well as in nonpolar solvents under an optimum acid concentration. Second, the relatively large molecular frame in the 3FAI dimer makes the high-level ab initio approach in the excited states very expensive and in some cases even formidable under the limit of our currently accessible computation resources. In comparison, the molecular framework of the 3FAI/formic acid hydrogen-bonding system is relatively much simpler than that of the 3FAI dimeric form, allowing a more accurate ab initio approach based on higher levels of theory. Finally, unlike the 7AI dimer and 7AI/alcohol complexes, the experimental difficulty in performing the real-time ESDPT dynamics of 3FAI (or 7AI)/carboxylic acid hydrogen-bonded complexes[46] makes the theoretical approach more intriguing and significant.

**3.2. Approaches in the Ground State.** Figure 2**a**−**c** and Table 1 specify several critical bond lengths at the stationary-point geometry in the ground and excited states calculated via various theoretical methods. For the ground-state reactant (i.e., the normal species), all Hartree−Fock methods predicted similar bond lengths except for the hydrogen-bonding distances R2 and R6 for which the HF/3-21G(d,p) method gave significantly shorter bond lengths (see Table 1). The B3LYP method also predicted shorter hydrogen bonds than those obtained from Hartree−Fock methods by approximately 0.2 Å using the same basis set (i.e., 6-31G(d′,p′)). Similar results were also found for the ground-state product (i.e., the proton-transfer tautomer) for which calculations based on the B3LYP/6-31G(d′,p′) method predicted significantly shorter R1 and R5 hydrogen-bonding lengths than those calculated using HF/6-31G(d′,p′). The difference between the B3LYP and HF is possibly due to the correlation energies incorporated in the DFT method, predicting a stronger hydrogen-bonding strength. Table 2 lists the ground-state energetics of the double proton-transfer reaction calculated for the 3FAI/formic acid complex at various theoretical levels. All calculations predicted the proton-transfer tautomer to be higher in energy than the normal form by 5−10 kcal/mol. In particular, the relative energy of the proton-transfer tautomerism was calculated to be 8.3 and 5.4 kcal/mol, respectively, at HF/6-31G(d′,p′) and B3LYP/6-31G(d′,p′) levels, which are consistent with the results obtained in the 7AI/water system based on similar methods.[34b] Incorporating the electron correlation reduces the energy difference. This viewpoint is supported by the similar tautomerization energy of 5.4 and 6.8 kcal/mol obtained at B3LYP/6-31G(d′,p′) and MP2/6-31G(d′,p′)//B3LYP/6-31G(d′,p′) levels, respectively. In comparison, independent of the basis sets, the energy difference between the normal and tautomer species in the ground state was estimated to be >8 kcal/mol at all Hartree−Fock levels.

Upon incorporating the electron correlation, a similar trend in the barrier height reduction was found in both the forward

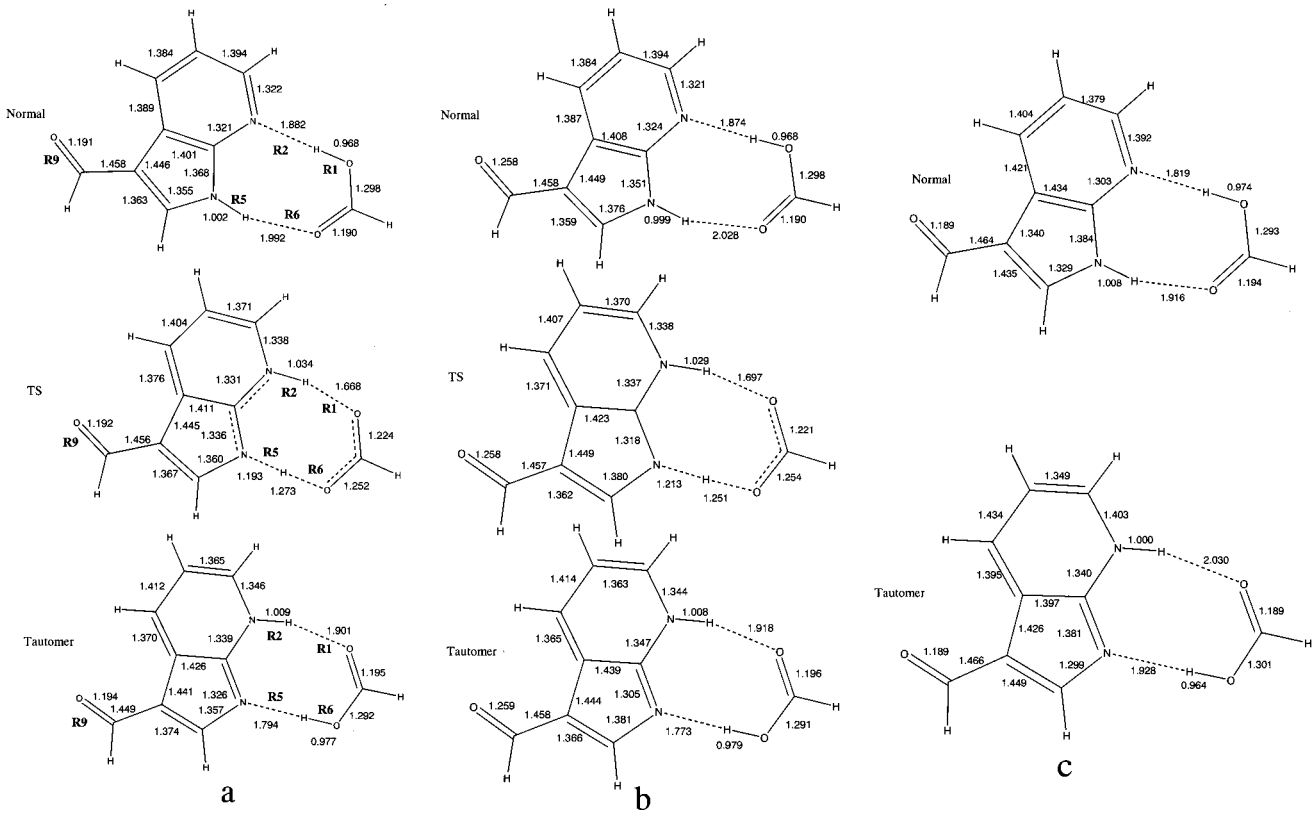


**Figure 2.** The calculated stationary point geometry at HF/6-31G(d′,p′) and CIS/6-31G(d′,p′) levels for normal, TS, and proton-transfer tautomer of the 3FAI/formic acid complex in (a) $S_0$, (b) $S_{n\pi^*}$, and (c) $S_{\pi\pi^*}$ states. The label of chemical bonds including the hydrogen bond is referred to that depicted in the $S_0$ state.

and reverse proton-transfer reactions. The calculated classical barrier height of the forward reaction, depending on various applied methods, ranges from 7 to 16 kcal/mol (see Table 2). Values obtained by B3LYP/6-31G(d′,p′) (7.3 kcal/mol) and MP2/6-31G(d′,p′)//B3LYP/6-31G(d′,p′) (9.9 kcal/mol) calculations are 6−8 kcal/mol lower than those predicted at the Hartree−Fock level using the same basis set. Similarly, the energy barrier of reverse proton transfer was calculated to be 1.9 and 3.1 kcal/mol at B3LYP and MP2 levels, while the Hartree−Fock method with the same basis set (i.e., 6-31G(d′,p′)) estimated an energy barrier of ∼7.8 kcal/mol for the reverse proton transfer. This discrepancy is believed to result mainly from the negligence of the electron correlation in the Hartree−Fock approach.

In consideration of the ground transition-state (TS) geometry, only the R1 value varies significantly among the various calculation methods (see Table 1 and Figure 2a). The results perhaps indicate that at the transition state, R1 is the only stable hydrogen bond remaining. This in combination with only one TS being resolved led us to conclude that the double proton transfer takes place through a concerted, asynchronous pathway in the ground state. At the TS, the carboxylic hydrogen on the formic acid has already been transferred to the pyridinic nitrogen, while the pyrrolic hydrogen has just begun to move toward the carbonyl oxygen of the formic acid. This prediction qualitatively correlates with the hydrogen-bonding strength predicted from the "acid−base" type of empirical approach.[47] Table 3 summarizes p$K_a$ values of various hydrogen-bonding sites for both 3FAI and acetic acid. Although these data were obtained in aqueous solution and acetic acid was used instead of formic acid, an interesting correlation is still observed between the sum of p$K_a$ (proton donor) and p$K_b$ (proton acceptor, p$K_b$ = p$K_{H_2O}$ − p$K_a$, where $K_{H_2O}$ is the autoprotolysis constant of $H_2O$) and the hydrogen-bonding site actively involved in the complex formation. For instance, in the case of a 1:1 3FAI/acetic acid complex, the value of p$K_a$ + p$K_b$ was calculated to be on the order of 3FAI(−N−)/acetic acid(−OH) ≪ 3FAI(−N−H)/acetic acid(=O). The sum of p$K_a$ and p$K_b$ is equivalent to $-\log K_{eq}$, where $K_{eq}$ denotes the equilibrium constant for the acid−base reaction. Hence, a lower p$K_a$ + p$K_b$ value indicates a large acid−base equilibrium constant and the reaction favors the product formation, i.e., the hydrogen-bond formation. Such an empirical approach predicts a stronger pyridinic nitrogen−carboxylic (−OH) hydrogen-bonding strength. When the TS is treated as an acid−base-type quasi-equilibrium, it is rational that the first-step proton transfer involving carboxylic hydrogen to the pyridinic nitrogen in 3FAI should be in the minimum energy pathway. It should also be noted that, independent of the applied basis sets, only one TS was found at both HF and B3LYP calculations. For a concerted, asynchronous double proton-transfer model, the results indicate that the proton transfer from carboxylic hydrogen is nearly barrierless. Nevertheless, there is no guarantee of the existence of more than one TS upon treatment with even higher-level calculations.

**3.3. Approaches in the Excited States.** At this stage, complete active space−self consistent field (CASSCF) calculations are not practical in dealing with the 3FAI/formic acid complex (vide infra). Alternatively, CIS is proven to be a relatively useful method to obtain the approximate wave function and molecular geometry of the electronic excited states. However, it usually overestimates the energy differences between the excited and ground states. In comparison, the time-dependent DFT method currently cannot perform geometry optimization at the excited states, but it has been shown to be able to obtain very reliable vertical excitation energies for the

**TABLE 1: Critical Bond Distances (Å) of 3FAI/Formic Acid Normal, TS, and Proton-Transfer Tautomer calculated by various methods in $S_0$, $S_{n\pi^*}$, and $S_{\pi\pi^*}$ States**

| | HF/3-21G(d,p) | HF/6-31G(d′) | HF/6-31G(d′,p′) | B3LYP/6-31G(d′,p′) |
|---|---|---|---|---|
| | | $S_0$ | | |
| | | Normal Form | | |
| R1 | 0.974 | 0.966 | 0.968 | 1.018 |
| R2 | 1.761 | 1.903 | 1.882 | 1.687 |
| R5 | 1.001 | 1.000 | 1.002 | 1.028 |
| R6 | 1.825 | 1.996 | 1.992 | 1.819 |
| R9 | 1.217 | 1.191 | 1.191 | 1.217 |
| | | TS Form | | |
| R1 | 1.539 | 1.732 | 1.668 | 1.513 |
| R2 | 1.038 | 1.024 | 1.034 | 1.090 |
| R5 | 1.240 | 1.223 | 1.193 | 1.229 |
| R6 | 1.212 | 1.241 | 1.273 | 1.267 |
| R9 | 1.219 | 1.193 | 1.192 | 1.220 |
| | | Tautomer Form | | |
| R1 | 1.736 | 1.913 | 1.901 | 1.720 |
| R2 | 1.013 | 1.007 | 1.009 | 1.043 |
| R5 | 1.663 | 1.828 | 1.794 | 1.594 |
| R6 | 0.990 | 0.974 | 0.977 | 1.040 |
| R9 | 1.220 | 1.195 | 1.194 | 1.222 |
| | CIS/3-21G(d,p) | CIS/6-31G(d′) | CIS/6-31G(d′,p′) | |
| | | $S_{n\pi^*}$ | | |
| | | Normal Form | | |
| R1 | 0.975 | 0.967 | 0.968 | |
| R2 | 1.759 | 1.895 | 1.874 | |
| R5 | 0.999 | 0.998 | 0.999 | |
| R6 | 1.847 | 2.030 | 2.028 | |
| R9 | 1.294 | 1.258 | 1.258 | |
| | | TS Form | | |
| R1 | 1.616 | 1.751 | 1.697 | |
| R2 | 1.032 | 1.021 | 1.029 | |
| R5 | 1.259 | 1.245 | 1.213 | |
| R6 | 1.194 | 1.224 | 1.251 | |
| R9 | 1.293 | 1.259 | 1.258 | |
| | | Tautomer Form | | |
| R1 | 1.748 | 1.926 | 1.918 | |
| R2 | 1.012 | 1.005 | 1.008 | |
| R5 | 1.647 | 1.811 | 1.773 | |
| R6 | 0.993 | 0.976 | 0.979 | |
| R9 | 1.294 | 1.259 | 1.259 | |
| | CIS/3-21G(d,p) | CIS/6-31G(d′) | CIS/6-31G(d′,p′) | |
| | | $S_{\pi\pi^*}$ | | |
| | | Normal Form | | |
| R1 | 0.984 | 0.971 | 0.974 | |
| R2 | 1.701 | 1.849 | 1.819 | |
| R5 | 1.010 | 1.005 | 1.008 | |
| R6 | 1.750 | 1.926 | 1.916 | |
| R9 | 1.217 | 1.189 | 1.189 | |
| | | Tautomer Form | | |
| R1 | 1.856 | 2.031 | 2.030 | |
| R2 | 1.000 | 0.998 | 1.000 | |
| R5 | 1.798 | 1.946 | 1.928 | |
| R6 | 0.968 | 0.962 | 0.964 | |
| R9 | 1.218 | 1.189 | 1.189 | |

low-lying excited states.[48] Accordingly, two ways of calculating the excited-state energies were employed here. The first approach was based on a vertical excitation in which the excited-state geometry was taken from the ground-state optimized structure. This was performed using the CIS level at the HF geometry or the TD-B3LYP level at HF and B3LYP geometry for both normal and tautomer forms. The other approach was to optimize the excited-state geometry directly at the CIS level followed by the vertical excitation using the TD-B3LYP method.

**TABLE 2: Proton-Transfer Energetics (kcal/mol) of 3FAI/Formic Acid in $S_0$, $S_{n\pi^*}$, and $S_{\pi\pi^*}$ States[a]**

| | $E_{rxn}$ | $\Delta V^{\ddagger}$ |
|---|---|---|
| | $S_0$ State | |
| HF/3-21G | 8.6 | 9.0 |
| HF/3-21G(d,p) | 9.6 | 13.6 |
| HF/3-21+G(d,p) | 8.4 | 10.9 |
| HF/6-31+G(d,p) | 8.2 | 15.1 |
| HF/6-31G(d′) | 8.4 | 16.6 |
| HF/6-31G(d′,p′) | 8.3 | 16.1 |
| B3LYP/6-31G(d′,p′) | 5.4 | 7.3 |
| MP2/6-31G(d′,p′)// B3LYP/6-31G(d′,p′) | 6.8 | 9.9 |
| | $S_{n\pi^*}$ | |
| Cis/3-21G(d,p) | 11.3 | 14.5 |
| Cis/6-31G(d′) | 10.3 | 17.3 |
| Cis/6-31G(d′,p′) | 10.2 | 16.7 |
| | $S_{\pi\pi^*}$ | |
| Cis/3-21G(d,p) | −14.2 | |
| Cis/6-31G(d′) | −14.8 | |
| Cis/6-31G(d′,p′) | −14.7 | |

[a] $E_{rxn}$ denotes the energy difference between 3FAI/formic acid normal and tautomer complexes. $\Delta V^{\ddagger}$ symbolizes the forward reaction energy barrier. The energies include electronic and nuclear repulsion energies; zero-point and thermal energies are not included.

**TABLE 3: p$K_a$ Values for Various Functional Groups in 3FAI and Acetic Acid**

| | 3FAI (−$NH^+$) | 3FAI (N−H) | ACID (−OH) | ACID (=$OH^+$) | ACID ($OH_2^+$) |
|---|---|---|---|---|---|
| p$K_a$ | 2.54[a] | 11.12[a] | 4.75[b] | −6.5[b] | ≤6.5[c] |

[a] Data were obtained by using the absortption titration study. [b] Gordon, A. J.; Ford, R. A. *The Chemist's Companion*; John Willey & Sons: New York, 1972. [c] Not available due to its stronger acidity than ACID(=$OH^+$).

**TABLE 4: The Low-Lying Singlet Electronic Transitions of Normal Form Calculated via TD-B3LYP and CIS Methods**

| transition | dominant configurations | $\tilde{\nu}$ ($cm^{-1}$) | oscillator strength (*f*) |
|---|---|---|---|
| | 3FAI/Formic Acid | | |
| | TD-B3LYP//B3LYP/6-31G(d′,p′) | | |
| $S_1(n \rightarrow \pi^*)$ | HOMO-1 → LUMO, LUMO + 1 | 31 292 | 0.0001 |
| $S_2(\pi \rightarrow \pi^*)$ | HOMO → LUMO, LUMO + 1 | 36 051 | 0.0542 |
| | CIS//HF/6-31G(d′,p′) | | |
| $S_1(n \rightarrow \pi^*)$ | HOMO-2 → LUMO, LUMO + 1 | 41 777 | 0.0003 |
| $S_2(\pi \rightarrow \pi^*)$ | HOMO-1, HOMO → LUMO | 47 100 | 0.2247 |
| | 7AI/Formic Acid | | |
| | TD-B3LYP//B3LYP/6-31G(d′,p′) | | |
| $S_1(\pi \rightarrow \pi^*)$ | HOMO-1 → LUMO + 1<br>HOMO → LUMO | 35 325 | 0.0463 |
| $S_2(\pi \rightarrow \pi^*)$ | HOMO-1 → LUMO<br>HOMO → LUMO + 1 | 38 905 | 0.0770 |

The calculation renders the absolute energies of the stationary points on the excited-state PES.

Table 4 lists the wave function properties of two low-lying singlet excited states and their associated transition from major molecular orbitals for the normal species. For clarity, Figure 3 depicts the structures of the two lowest unoccupied and three (CIS level) or two (TD-B3LYP level) highest occupied frontier molecular orbitals mainly involved in the transition of low-lying excited states using either the CIS//HF/6-31G(d′,p′) or TD-B3LYP//B3LYP/6-31G(d′,p′) method. Depending on the levels of theory, the calculations differ slightly in the nature of the molecular orbitals involved in the predominant excitations. For example, the $S_2$ state is a contribution from HOMO → LUMO, LUMO+1 in the TD-B3LYP calculations versus HOMO-1,

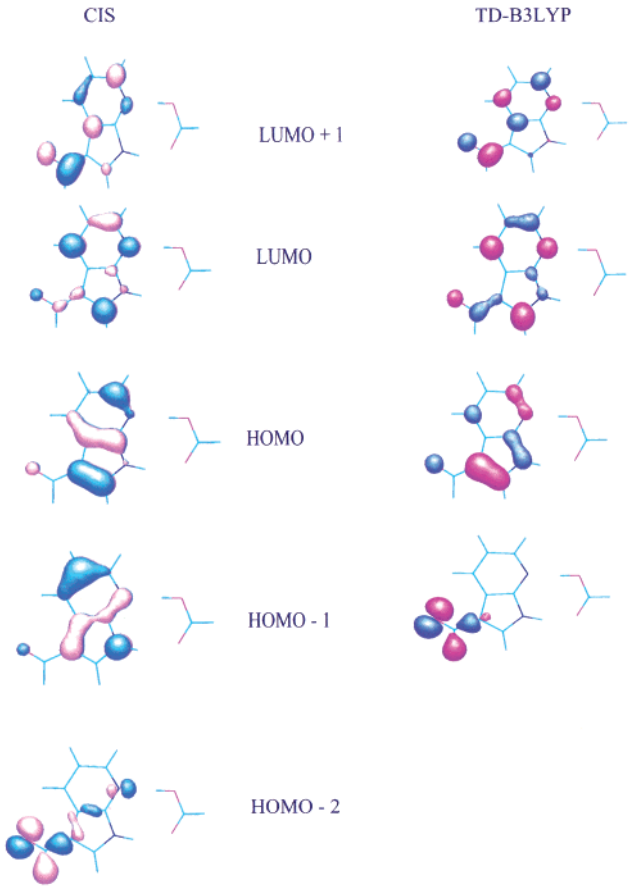


**Figure 3.** The calculated (CIS//HF/6-31G(d′,p′) and TD-B3LYP//B3LYP/6-31G(d′,p′)methods) frontier molecular orbitals for the normal form of the 3FAI/formic acid complex. Note that the orbital configuration of HOMO-1 obtained using the TD-B3LYP method is essentially the same as that of HOMO-2 obtained using the CIS method.

**TABLE 5: Calculated Vertical Excitation Energies (eV) of the 3FAI/Formic Acid Complex via Various Methods**

| normal form | | tautomer form | |
|---|---|---|---|
| nπ* | ππ* | nπ* | ππ* |
| TD-B3LYP//HF/6-31G(d′,p′) | | | |
| 4.05 | 4.66 | 3.80 | 3.61 |
| TD-B3LYP//B3LYP/6-31G(d′,p′) | | | |
| 3.88 | 4.47 | 3.73 | 3.59 |
| CIS//HF/6-31G(d′,p′) | | | |
| 5.18 | 5.84 | 5.26 | 5.02 |

HOMO → LUMO in the CIS computations. Nevertheless, both methods predicted a similar trend that the $S_1$ and $S_2$ states in the 3FAI/formic acid complex can be well ascribed using a forbidden n ($\sigma$-symmetry) → $\pi^*$ ($\pi$-symmetry) and an allowed ($\pi$-symmetry) → $\pi^*$ ($\pi$-symmetry) transition, respectively, in which the nonbonding orbital is largely attributed to the carbonyl oxygen in the formyl substituent. In contrast, as shown in Table 4, the first two low-lying excited singlet states for the 7AI/formic acid complex are unambiguously ascribed to the $\pi\pi^*$ configuration. The $n\pi^*$ state of the 7AI/formic acid complex in which the nonbonding orbital is ascribed to the pyridinic nitrogen was calculated to be in the highly excited $S_5$ state (not shown here).

The calculated vertical excited-state energies using CIS and TD-B3LYP methods for both 3FAI normal and tautomer/formic acid species are listed in Table 5. Independent of the applied methods and basis sets the $^1n\pi^*$ state is predicted to be lower in energy than the $^1\pi\pi^*$ state for the normal form, while the order is reversed for the tautomer/formic acid complex. With the use of the TD-B3LYP method incorporating the B3LYP geometry, the vertical excitation energy from the ground-state normal form to the $^1\pi\pi^*$ state was calculated to be 4.47 eV (36 050 $cm^{-1}$), which is consistent with the experimentally determined ~4.13 eV (33 308 $cm^{-1}$ [37]) for the first $\pi\pi^*$ singlet excited state. On the basis of the Hartree−Fock geometry, the $^1n\pi^*$ state was predicted to be 5.18 and 4.05 eV above the ground state at the CIS and TD-B3LYP levels, respectively. If the B3LYP geometry is used instead, the TD-B3LYP method predicted an excitation energy gap of 3.88 eV for the $^1n\pi^*$ state. Experimentally, the extremely small absorption cross section (i.e., the molar extinction coefficient) for the orbital forbidden n → $\pi^*$ transition led to an infeasible spectroscopic measurement. Nevertheless, under the circumstance that the $^1n\pi^*$ state is lower in energy than its close-lying $^1\pi\pi^*$ state, the n → $\pi^*$ transition is predicted to be <4.13 eV. Accordingly, the TD-B3LYP method with the B3LYP geometry incorporated renders more reliable single-point energetics for the low-lying excited states. Even though CIS and TD-B3LYP methods predicted significantly different vertical excitation energies, the calculated relative energy gaps between $^1n\pi^*$ and $^1\pi\pi^*$ states are on a similar trend. For example, the CIS excitation energy calculation estimated the $^1\pi\pi^*$ state to be 0.66 eV above the $^1n\pi^*$ state at the normal form, which is only 0.05 eV higher than the difference between $^1\pi\pi^*$ and $^1n\pi^*$ states estimated using the TD-B3LYP method under the same HF ground-state geometry.

In consideration of the excitation energetics of the proton-transfer tautomer, a better comparison with spectroscopic (i.e., fluorescence) data would be using the CIS-optimized geometry for the excited state and, alternatively, performing the vertical excitation on the basis of the TD-B3LYP method. The energy gap between $^1\pi\pi^*$ and the ground state for the 3FAI(tautomer)/formic acid complex was calculated to be 2.80 eV (22 582 $cm^{-1}$), which is consistent with the experimental value of ~2.76 eV (22 222 $cm^{-1}$) estimated from the proton-transfer tautomer emission in the case of the 3FAI/acetic acid complex.[37] We then made a further attempt to obtain information based on the CASSCF calculations. Normally, CASSCF only incorporates a static electron correlation, while the dynamic correlation is neglected. This disadvantage has been significantly improved through the incorporation of perturbation methods, i.e., with electron correlation (e.g., see ref 34b). Unfortunately, this method is not feasible at this stage under the limit of our current computing capacity.

Similar to the ground-state calculation, in comparison to the 3-21G(d,p) basis sets, the 6-31G(d′) and 6-31G(d′,p′) basis sets gave longer bond lengths (0.1−0.2 Å) for R2 and R6 at normal and R1 and R5 at tautomer forms in the excited states (see Table 1). Inclusion of the hydrogen polarization function (6-31G(d′,p′)) resulted in slightly (<0.03 Å) shorter distances of these bonds. Because the trends in geometry differences among the various stationary points are reproduced in all calculations, the discussion on molecular geometry in the rest of this paper will be based on the calculation with the 6-31G(d′,p′) basis set. Compared to their corresponding ground-state geometry, both the normal and tautomer forms in the $^1n\pi^*$ configuration have a much longer (~0.07 Å) C═O bond (R9), indicating that the nonbonding orbital on the oxygen actually stabilizes the C═O bond in the ground state. Promoting the lone-pair electron to the $\pi^*$ orbital decreases the C═O bond order and hence weakens the bonding energy. Other bond-distance changes in the rings or hydrogen-bonding network are much smaller (<0.02 Å). Conversely, for the $^1\pi\pi^*$ normal and tautomer species config-

uration, changes in the bond distance relative to their corresponding ground states are mainly located on the hydrogen bonds and, to a lesser extent, on the rings. In particular, the hydrogen-bonding distance between the pyridinic nitrogen and carboxylic hydrogen (i.e., R6) decreases by 0.08 Å in the $^1\pi\pi^*$ state at the normal species, indicating a stronger hydrogen-bonding formation upon the $\pi \rightarrow \pi^*$ excitation of the 3FAI/formic acid complex, which may subsequently initiate the proton-transfer reaction (vide infra).

We have made an attempt to locate the proton-transfer reaction pathway along the $^1\pi\pi^*$ electronic state via scanning the PES. According to the analysis of the TS structure in the ground state, it seems that the change in the bond distance at the COOH··· N(7) hydrogen-bonding site (see Figure 1 for the definition) is faster than that at the C═O···HN(1) site (vide supra). A two-dimensional scan of the PES in the $^1\pi\pi^*$ configuration is extremely time-consuming and hence is not feasible at this stage. Alternatively, we assumed a similar trend that the first proton-transfer process (i.e., COOH···N(7) → C═O···HN(7)) is relatively fast in the $^1\pi\pi^*$ state and simply scanned the C═O···HN(1) hydrogen-bonding distance by reducing 0.1 Å in each step. Simultaneously, we allowed a full optimization on the remaining bond angles and distances in the $^1\pi\pi^*$ configuration. At the CIS/3-21G(d,p) level, the results show a small barrier of 3.8 kcal/mol relative to the $^1\pi\pi^*$ normal form. The TS was confirmed by performing a full geometry optimization in which the geometry is closely related to the reactant, i.e., the 3FAI(normal)/formic acid complex. However, the barrier disappeared when a higher basis set of 6-31G(d′,p′) was applied (see Figure 4). It should be noted that the CIS method only includes a small fraction of the correlation energy.[41] However, higher-level correlation methods usually reduce the energy barrier if it exists. We also performed the energy profile calculations using the TD-B3LYP method on the reaction pathway that was initially scanned at the CIS/6-31G(d′,p′) level. The result revealed no energy barrier as well. Similar nonexistence of the energy barrier was obtained by scanning the PES on the COOH···N(7) → C═O···HN(7) hydrogen transfer process using the CIS/6-31G(d′,p′) method. Thus, no significant barrier of ESDPT seems to exist in the $^1\pi\pi^*$ electronic state when the calculation is performed via higher levels of theory (e.g., CIS/6-31G(d′,p′)).

We, however, were able to locate the ESDPT TS for the 3FAI/formic acid complex in the $^1n\pi^*$ configuration, and the energy barrier was found to be 16.7 kcal/mol above the normal form of the $^1n\pi^*$ state. The geometry of the $^1n\pi^*$ TS is similar to that of the ground TS except for a significantly longer bond distance (∼0.07 Å) in R9 (i.e., the C═O bond length), slightly longer bond distances (0.02−0.03 Å) in R1 and R5, and a shorter bond distance (∼0.02 Å) in R6. Figure 4 depicts the proton-transfer potential energy surfaces in $S_0$, $S_{n\pi^*}$ and $S_{\pi\pi^*}$ states for the 3FAI/formic acid complex, in which the horizontal thick line denotes the energy level at each stationary point geometry and the vertical dashed arrows indicate the vertical transition from the geometry optimized ground-state structure. The vertical solid line represents the tautomer emission resulting from the vertical transition at the geometry-optimized (the CIS method) $^1\pi\pi^*$ tautomer state. All vertical transitions were calculated using the TD-B3LYP method. Note that the PES depicted in Figure 4 is qualitative, and one must keep in mind that the actual landscape of potential energy surfaces should be multidimensional.

**3.4. Comparison with Experimental Results.** The results of small barrier for the ground-state reverse proton transfer

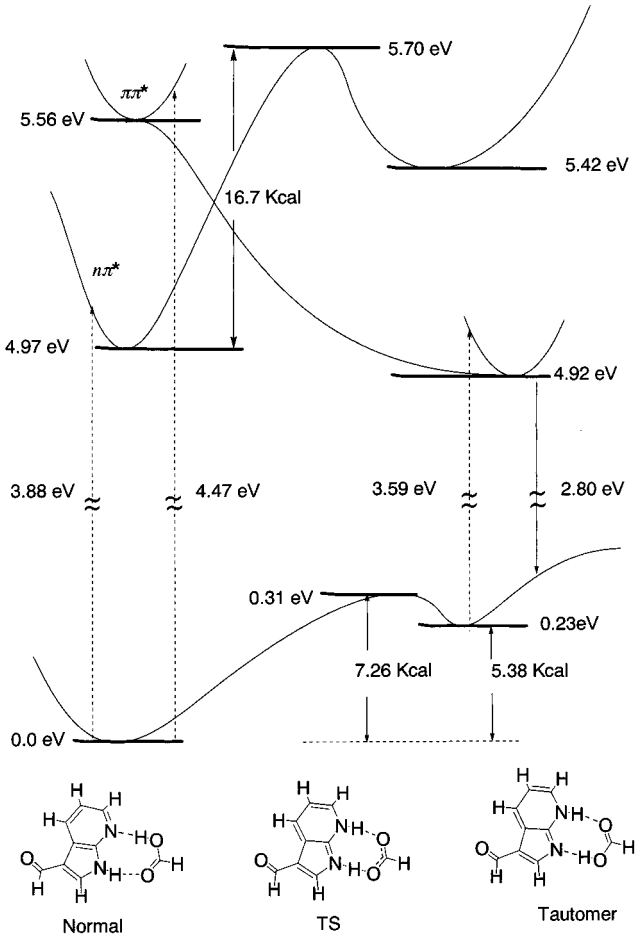


**Figure 4.** A qualitative sketch of potential energy surfaces for the proton-transfer reaction in $S_0$, $S_{n\pi^*}$, and $S_{\pi\pi^*}$ states based on the calculated reactant, TS, and product energies (see text for the detailed description). The relative energies depicted in the ground state were obtained using the B3LYP/6-31G(d′,p′) method.

suggest that following the ESDPT the ground-state tautomer complex produced via the deactivation of the excited state may quickly undergo reverse proton transfer to the normal form. Experimentally, on the basis of a two-step laser-induced fluorescence (TSLIF) technique,[17] an attempt to resolve the transient ground-state tautomer species in the 3FAI/acetic acid complex was made. The results of no TSLIF signal being detected at >10 ns pump−probe delay time led us to conclude that the rate of ground-state reverse proton transfer should be faster than the decay rate (∼$9 \times 10^7$ $s^{-1}$ [37]) of the excited 3FAI-(tautomer)/formic acid complex. Consequently, the overall rate of a proton cycle is mainly limited by the relaxation dynamics of the tautomer emission, consistent with the theoretical approach.

On the basis of the calculated highly exergonic, barrierless reaction in the $^1\pi\pi^*$ state, one should come up with the following dynamic viewpoint. The rapid charge redistribution after first singlet $\pi \rightarrow \pi^*$ excitation results in an electronic potential surface possessing substantial slope and an energy minimum shift toward the proton position in the imine-like tautomer. The redistribution of the electronic charge is expected to occur on a time scale much shorter than 100 fs. Some of the normal modes of the molecule are now displaced from their equilibrium positions that are determined by the new potential surface. As a result, the excited system begins to evolve temporally along these normal coordinates, i.e., it moves on the excited-state energy surface toward the new equilibrium

position. Especially any normal coordinate connected with the proton displacement deviates strongly from its equilibrium position, which is reached by the formation of the excited proton-transfer tautomer. The system energy, after being redistributed, is then seeking an exit. Most probably, the low-frequency, large-amplitude modes (e.g., either in- or out-of-plane motions of the skeletal modes) change the relative position of the atoms associated with the hydrogen bond and hence channel into the proton-transfer process. In this case, deuterium isotope substitution should have a negligible effect on the observed ESDPT dynamics. This apparently is not the case in studying the 7AI dimer in gas[12] as well as in the nonpolar solvents[14−16] in which a small energy barrier is associated with the proton transfer reaction and a prominent deuterium isotope effect was observed. In the case of the 3FAI/acetic acid complex, a deuterium isotope effect was also observed in a steady-state approach.[37]As pointed out earlier, on one hand, there may exist a nonnegligibly small energy barrier (i.e., the existence of a TS in the case of the 3FAI/acetic acid in the $^1\pi\pi^*$ configuration), which unfortunately cannot be resolved on the basis of the current computation methods. On the other hand, through vibronic coupling, state mixing between the two close-lying $^1\pi\pi^*$ and $^1$n$\pi^*$ configurations is possible, resulting in a small barrier for the proton-transfer reaction. Geometry optimization at the CIS level resulted in the stationary point energy differences of 0.59 eV (13.6 kcal/mol) between the $\pi\pi^*$ and n$\pi^*$ states for the normal form. However, calculations regarding this viewpoint were not performed in this study because of the complexity of the molecular framework as well as the lack of information on the solvent perturbation. Furthermore, the previous report of the deuterium isotope effect on the rate of ESDPT (i.e., $k_{pt}^{H} \sim 2k_{pt}^{D}$) was deduced from a steady state approach in which both the radiative and nonradiative decay rates of the tautomer emission were assumed to be deuterium-isotope-independent.[37] Therefore, the interpretation of deuterium isotope dependence may be subject to certain uncertainties. Further direct verification of the ESDPT dynamics in 3FAI (or 3AI)/acetic acid systems should rely on the time-resolved measurement with femtosecond resolution. Focus on this issue is currently in progress.

Finally, according to the barrier height of 16.7 kcal/mol, ESDPT in the $^1$n$\pi^*$ configuration is concluded to be dynamically prohibited within the life span of the $^1$n$\pi^*$ state. Experimentally, the decay rate of the non-proton-transfer channels of the $^1$n$\pi^*$ state was estimated to be $\gg 30$ ns$^{-1}$ through the transient absorption study.[37] The fast depopulation of the $^1$n$\pi^*$ state, resulting in a lack of fluorescence, may be tentatively rationalized by the fast $^1$n$\pi^* \rightarrow {}^3\pi\pi^*$ system crossing. Evidence has been provided by observation of the significant triplet−triplet transient absorption spectra,[37] although a quantitative study of the triplet yield has not yet been performed. In an extreme case, the corresponding pseudo-Jahn−Teller distortion may be incorporated because of the proximity between the $^1$n$\pi^*$ and $^1\pi\pi^*$ states, enhancing a nonradiative decay channel. Such a mechanism requires the molecule to be distorted along a nontotally symmetric (i.e., out-of-plane) coordinate and has been proposed to explain the dominant nonradiative pathways in adenine and its derivatives associated with the torsional motion of the (alkyl)-amino substituents.[49−51] In the case of 3FAI, twisting the exocyclic formyl group certainly associates with a nontotally symmetric distortion. We have recently synthesized and studied various 6-alkylamino-7-azaindoles to test the nonradiative mechanism incorporating the twisting of the alkylamino substituents. The results will be published in a forthcoming paper.

## Conclusion

The results based on various ab initio methods are qualitatively consistent, showing that the lowest singlet excited state in the 3FAI/formic acid complex is in an n$\pi^*$ configuration. This transition originates from the carbonyl lone-pair electron in the 3-formyl substituent, as was supported by the molecular orbital analyses and a comparative study with respect to the 7AI/formic acid hydrogen-bonded complex. In contrast to the calculated barrierless ESDPT in the $^1\pi\pi^*$ state, a highly endergonic proton-transfer reaction was deduced in the $^1$n$\pi^*$ state. As a result, upon $^1\pi\pi^*$ excitation, a competitive mechanism[37] incorporating the rate of $^1\pi\pi^* \rightarrow {}^1$n$\pi^*$ internal conversion versus the proton-transfer reaction rate should be operative. ESDPT is prohibited in the $^1$n$\pi^*$ state of which the decay dynamics are dominated by intersystem crossing or other non-proton-transfer radiationless transitions or both.

**Acknowledgment.** This work was supported by the National Science Council, Taiwan, ROC (Grant NSC89-2113-M-194-009). We thank the National Center for High-Performance Computing, Taiwan, for the use of their facility.

## References and Notes

(1) Taylor, C. A.; El-Bayoumi, A. M.; Kasha, M. *Proc. Natl. Acad. Sci. U.S.A.* **1969**, *65*, 253.
(2) Ingham, K. C.; El-Bayoumi, M. A. *J. Am. Chem. Soc.* **1971**, *93*, 5023.
(3) Ingham, K. C.; El-Bayoumi, M. A. *J. Am. Chem. Soc.* **1974**, *96*, 1674.
(4) Watson, J. D.; Crick, F. H. C. *Nature (London)* **1953**, *171*, 964.
(5) Watson, D. G.; Sweet, R. M.; Marsh, R. E. *Acta Crystallogr.* **1965**, *19*, 573.
(6) Hetherington, W. M., III; Micheels, R. H.; Eisenthal, K. B. *Chem. Phys. Lett.* **1979**, *66*, 230.
(7) Fuke, K.; Yoshiuchi, H.; Kaya, K. *J. Phys. Chem.* **1984**, *88*, 5840.
(8) Waluk, J.; Herbich, J.; Oelkrug, D.; Uhl, S. *J. Phys. Chem.* **1986**, *90*, 3866.
(9) Fuke, K.; Kaya, K. *J. Phys. Chem.* **1989**, *93*, 614.
(10) Tokumura, K.; Watanabe, Y.; Udagawa, M.; Itoh, M. *J. Am. Chem. Soc.* **1987**, *109*, 1346.
(11) Share, P.; Pereira, M.; Sarisky, M.; Repinec, S.; Hochstrasser, R. M. *J. Lumin.* **1991**, *48/49*, 204.
(12) Douhal, A.; Kim, S. K.; Zewail, A. H. *Nature* **1995**, *378*, 260.
(13) Folmer, D. E.; Poth, L.; Wisniewski, E. S.; Castleman, A. W., Jr. *Chem. Phys. Lett.* **1998**, *287*, 1.
(14) Chachisvillis, M.; Fiebig, T.; Douhal, A.; Zewail, A. H. *J. Phys. Chem. A* **1998**, *102*, 669.
(15) Takeuchi, S.; Tahara, T. *J. Phys. Chem. A* **1998**, *102*, 7740.
(16) Fiebig, T.; Chachisvillis, M.; Manger, M.; Zewail, A. H.; Douhal, A.; Garcia Ochoa, I.; de La Hoz Ayuso, A. *J. Phys. Chem. A* **1999**, *103*, 7419.
(17) Chou, P. T.; Yu, W. S.; Chen, Y. C.; Wei, C. Y.; Martinez, S. S. *J. Am. Chem. Soc.* **1998**, *120*, 12927.
(18) Bulska, G.; Grabowska, A.; Pakula, B.; Sepiol, J.; Waluk, J.; Wild, U. P. *J. Lumin.* **1984**, *29*, 65.
(19) Douhal, A.; Guallar, V.; Moreno, M.; Lluck, J. M. *Chem. Phys. Lett.* **1996**, *256*, 370.
(20) Guallar, V.; Moreno, M.; Lluch, J. M. *Chem. Phys. Lett.* **1998**, *228*, 1.
(21) Gullar, V.; Batista, V.; Miller, W. H. *J. Chem. Phys.* **1999**, *110*, 9922.
(22) Kim, S. K.; Bernstein, E. R. *J. Phys. Chem.* **1990**, *94*, 3531.
(23) Ilich, P. *J. Mol. Struct.* **1995**, *354*, 37.
(24) Shukla, M. K.; Mishra, P. C. *Chem. Phys.* **1998**, *230*, 187.
(25) Catalan, J.; Del Valle, J. C.; Kasha, M. *Proc. Natl. Acad. Sci. U.S.A.* **1999**, *96*, 8338.
(26) Catalan, J.; Kasha, M. *J. Phys. Chem. A* **2000**, *104*, 10812.
(27) Fiebig, T.; Chachisvilis, M.; Manger, M.; Zewail, A. H.; Douhal, A.; Garcia-Ochoa, I.; de La Hoz Ayuso, A. *J. Phys. Chem. A* **1999**, *103*, 7419.
(28) McMorrow, D.; Aartsma, T. *Chem. Phys. Lett.* **1986**, *125*, 581.
(29) Moog, R. S.; Bovino, S. C.; Simon, J. D. *J. Phys. Chem.* **1988**, *92*, 6545.
(30) Koijnenberg, J.; Huizer, A. H.; Varma, C. A. O. *J. Chem. Soc., Faraday Trans. 2* **1988**, *84* (8), 1163.

(31) (a) Moog., R. S.; Maroncelli, M. *J. Phys. Chem*. **1991**, *95*, 10359. (b) Chapman, C. F.; Maroncelli, M. *J. Phys. Chem.* **1992**, *96*, 8430. (c) Mentus, S.; Maroncelli, M. *J. Phys. Chem. A* **1998**, *102*, 3860.

(32) (a) Negreie, M.; Bellefeuille, S. M.; Whitham, S.; Petrich, J. W.; Thornburg, R. W. *J. Am. Chem. Soc.* **1990**, *112*, 7419. (b) Negrerie, M.; Gai, F.; Bellefeuille, S. M.; Petrich, J. W. *J. Phys. Chem.* **1991**, *95*, 8663. (c) Negrerie, M.; Gai, F.; Lambry, J.-C.; Martin, J.-L.; Petrich, J. W. *J. Phys. Chem.* **1993**, *97*, 5046. (d) Chen, Y.; Rich, R. L.; Gai, F.; Petrich, J. W. *J. Phys. Chem*. **1993**, *97*, 1770. (e) Chen, Y.; Gai, F.; Petrich, J. W. *J. Am. Chem. Soc.* **1993**, *115*, 10158. (f) Rich, R. L.; Chen, Y.; Neven, D.; Negrerie, M.; Gai, F.; Petrich, J. W. *J. Phys. Chem.* **1993**, *97*, 1781. (g) Gai, F.; Rich, R. L.; Petrich, J. W. *J. Am. Chem. Soc*. **1994**, *116*, 735. (h) Smirnov, A. V.; English, D. S.; Rich, R. L.; Lane, J. Teyton, L.; Schwabacher, A. W.; Luo, S.; Thornburg, R. W.; Petrich, J. W. *J. Phys. Chem.* **1997**, *101B*, 2758 and references therein.

(33) (a) Chou, P. T.; Martinez, M. L.; Cooper, W. C.; McMorrow, D.; Collin, S. T.; Kasha, M. *J. Phys. Chem*. **1992**, *96*, 5203. (b) Chang, C. P.; Hwang, W. C.; Kuo, M. S.; Chou, P. T.; Clement, J. H. *J. Phys. Chem.* **1994**, *98*, 8801. (c) Chou, P. T.; Wei, C. Y.; Chang, C. P.; Chiu, C. H. *J. Am. Chem. Soc.* **1995**, *117*, 7259. (d) Chou, P. T.; Wei, C. Y.; Chang, C. P.; Kuo, M. S. *J. Phys. Chem.* **1995**, *99*, 11994. (e) Chou, P. T.; Yu, W. S.; Wei, C. Y.; Chen, Y. M.; Yang, C. Y. *J. Am. Chem. Soc.* **2001**, *123*, 3599.

(34) (a) Gordon, M. S. *J. Phys. Chem*. **1996**, *100*, 3974. (b) Chaban, G. M.; Gordan, M. S. *J. Phys. Chem. A* **1999**, *103*, 185.

(35) (a) Fernández-Ramos, A.; Smedarchina, Z.; Siebrand, W.; Zgierski, M. Z.; Rios, M. A. *J. Am. Chem. Soc.* **1999**, *121*, 6280. (b) Smedarchina, Z.; Siebrand, W.; Fernández-Ramos, A.; Gorb, L.; Leszczynski, J. *J. Chem. Phys.* **2000**, *112*, 566.

(36) Kyrychenko, A.; Stepanenko, Y.; Waluk, J. *J. Phys. Chem. A* **2000**, *104*, 9542.

(37) Chou, P. T.; Wu, G. R.; Wei, C. Y.; Shiao, M. Y.; Liu, Y. I. *J. Phys. Chem. A* **2000**, *104*, 8863.

(38) Hehre, W. J.; Radom, L.; Schleyer, P. v. R.; Pople, J. A. *Ab Initio Molecular Orbital Theory*; John Wiley & Sons: New York, 1986.

(39) (a) Szabo, A.; Ostlund, N. S. *Modern Quantum Chemistry*; McGraw-Hill: New York, 1989 and references therein. (b) Foresman, J. B.; Frisch, A. *Exploring Chemistry with Electronic Structure Methods*, 2nd ed.; Gaussian Inc.: Pittsburgh, PA, 1996.

(40) Foresman, J. B.; Head-Gordon, M.; Pople, J. A.; Frisch, M. J. *J. Phys. Chem.* **1992**, *96*, 135.

(41) Frisch, M. J.; Trucks, G. W.; Schlegel, H. B.; Scuseria, G. E.; Robb, M. A.; Cheeseman, J. R.; Zakrzewski, V. G.; Montgomery, J. A., Jr.; Stratmann, R. E.; Burant, J. C.; Dapprich, S.; Millam, J. M.; Daniels, A. D.; Kudin, K. N.; Strain, M. C.; Farkas, O.; Tomasi, J.; Barone, V.; Cossi, M.; Cammi, R.; Mennucci, B.; Pomelli, C.; Adamo, C.; Clifford, S.; Ochterski, J.; Petersson, G. A.; Ayala, P. Y.; Cui, Q.; Morokuma, K.; Malick, D. K.; Rabuck, A. D.; Raghavachari, K.; Foresman, J. B.; Cioslowski, J.; Ortiz, J. V.; Stefanov, B. B.; Liu, G.; Liashenko, A.; Piskorz, P.; Komaromi, I.; Gomperts, R.; Martin, R. L.; Fox, D. J.; Keith, T.; Al-Laham, M. A.; Peng, C. Y.; Nanayakkara, A.; Gonzalez, C.; Challacombe, M.; Gill, P. M. W.; Johnson, B. G.; Chen, W.; Wong, M. W.; Andres, J. L.; Head-Gordon, M.; Replogle, E. S.; Pople, J. A. *Gaussian 98*, revision A.7; Gaussian, Inc.: Pittsburgh, PA, 1998.

(42) Petersson, G. A.; Al-Laham, M. A. *J. Chem. Phys.* **1991**, *94*, 6081.

(43) Becke, A. D. *J. Chem. Phys.* **1993**, *98*, 5648.

(44) (a) Lee, C.; Yang, W.; Parr, R. G. *Phys. Rev. B* **1988**, *37*, 785. (b) Miehlich, B.; Savin, A.; Stoll, H.; Preuss, H. *Chem. Phys. Lett.* **1989**, *157*, 200.

(45) (a) Bauernschmitt, R.; Ahlrichs, R. *Chem. Phys. Lett.* **1996**, *256*, 454. (b) Casida, M. E.; Jamorski, C.; Casida, K. C.; Salahub, D. R. *J. Chem. Phys.* **1998**, *108*, 4439.

(46) Despite profound time-resolved data on the 7AI dimer, detailed ESDPT dynamics on other host/guest complexes have not yet been explored. In our experience, the lack of dynamical information might be in part due to the complication in preparing an optimum concentration of host/guest complexes to perform the ultrafast time-resolved measurements. Concentrated 7AI (and its corresponding analogues) results in an appreciable dimeric formation, which undergoes a competitive equilibrium with respect to the host/guest complex. One may consider adding excess acetic acid concentration to shift the equilibrium toward the complex formation. Unfortunately, the accumulation of a local polarity due to the aggregation of acetic acid leads to the excited-state protonation rather than double proton-transfer reaction.

(47) Chou, P. T.; Wei, C. Y.; Wang, C. R. C.; Hung, F. T.; Chang, C. P. *J. Phys. Chem. A* **1999**, *103*, 1939.

(48) Full, J.; González, L.; Daniel, C. *J. Phys. Chem. A* **2001**, *105*, 184.

(49) Lai, T.; Lim, E. C. *Chem. Phys. Lett.* **1979**, *62*, 507.

(50) Lim, E. C. *J. Phys. Chem.* **1986**, *90*, 6770.

(51) Madej, S. L.; Okajima, S.; Lim, E. C. *J. Chem. Phys.* **1976**, *65*, 1219.